Applied Energy 190 (2017) 574–590

Contents lists available at ScienceDirect

Applied Energy

journal homepage: www.elsevier.com/locate/apenergy

A regenerative supercritical-subcritical dual-loop organic Rankine cycle system for energy recovery from the waste heat of internal combustion engines

Enhua Wang [a], Zhibin Yu [a,*], Hongguang Zhang [b], Fubin Yang [b]

[a] School of Engineering, University of Glasgow, Glasgow G12 8QQ, UK
[b] College of Environmental and Energy Engineering, Beijing University of Technology, Beijing 100124, China

HIGHLIGHTS

- A dual-loop ORC system using R1233zd and R1234yf is proposed.
- The performance of the system with different working fluids has been analysed.
- The integrated ICE-ORC system has been analysed.
- The off-design performance has been analysed.

ARTICLE INFO

Article history:
Received 20 August 2016
Received in revised form 16 December 2016
Accepted 27 December 2016

Keywords:
Supercritical organic Rankine cycle
Dual loop
Waste heat recovery
Environmentally friendly working fluid
CNG engine
Off-design performance

ABSTRACT

Organic Rankine cycle (ORC) system is considered as a promising technology for energy recovery from the waste heat rejected by internal combustion (IC) engines. However, such waste heat is normally contained in both coolant and exhaust gases at quite different temperatures. A single ORC system is usually unable to efficiently recover energy from both of these waste heat sources. A dual loop ORC system which essentially has two cascaded ORCs to recover energy from the engine's exhaust gases and coolant separately has been proposed to address this challenge. In this way, the overall efficiency of energy recovery can be substantially improved. This paper examines a regenerative dual loop ORC system using a pair of environmentally friendly refrigerants, R1233zd and R1234yf, as working fluids, to recover energy from the waste heat of a compressed natural gas (CNG) engine. Unlike most previous studies focusing on the ORC system only, the present research analyses the ORC system and CNG engine together as an integrated system. As such, the ORC system is analysed on the basis of real data of waste heat sources of the CNG engine under various operational conditions. A numerical model is employed to analyse the performances of the proposed dual loop cycle with four pairs of working fluids. The effects of a regenerative heat exchanger and several other key operating parameters are also analysed and discussed in detail. The performance of the integrated engine-ORC system is then analysed under actual engine operating conditions which were measured beforehand. The performance of the proposed system under off-design conditions has also been analysed. The obtained results show that the proposed dual loop ORC system could achieve better performance than other ORC systems for similar applications.

1. Introduction

Internal combustion (IC) engines are still the main power sources for transportation nowadays, and their dominance will not be changed in the foreseeable future. Over half of the energy contained in the fuel consumed by IC engines is ultimately discharged to the environment as waste heat via their cooling and exhaust systems. The energy efficiency of IC engines can be improved using waste heat recovery technologies such as organic Rankine cycle (ORC) systems [1], thermoelectric power generators [2], and combined heat and power (CHP) systems [3]. In the past decade or so, there has been a rapid increase of patent applications in the area of waste heat recovery technologies [4]. Such waste heat recovery systems could substantially improve the IC engine's overall thermal efficiency. For instance, Agudelo et al. evaluated the potential of exhaust heat recovery from a diesel engine of a

* Corresponding author.
E-mail address: Zhibin.Yu@glasgow.ac.uk (Z. Yu).

http://dx.doi.org/10.1016/j.apenergy.2016.12.122
0306-2619/© 2017 The Authors. Published by Elsevier Ltd.

Nomenclature

P	pressure (MPa)
$\dot{Q}$	heat quantity (kW)
SP	size parameter (cm)
T	temperature (K)
V	volume flow rate (m^3/s)
VFR	volume flow ratio
$\dot{W}$	power (kW)
h	enthalpy (kJ/kg)
$\dot{m}$	mass flow rate (kg/s)
s	entropy (kJ/kg·K)
Greek letters	
η	efficiency
ψ	performance improvement
Subscript	
HTi	state points in the HT loop
LTi	state points in the LT loop
abs	absolute change
c	condenser
$comb$	engine-DORC combined system
$cool$	coolant
$e1$	Evaporator 1
$e2$	Evaporator 2
eng	engine
exh	exhaust gas
f	fuel
in	inlet
is	isentropic
lm	logarithmic mean temperature difference
n	net
out	outlet
$p1$	Pump 1
$p2$	Pump 2
pre	preheater
$r1$	Regenerator 1
$r2$	Regenerator 2
rel	relative change
s	superheater
$t1$	Turbine 1
$t2$	Turbine 2
th	thermal efficiency
Acronyms	
CNG	compressed natural gas
DORC	dual-loop organic Rankine cycle
HT	high temperature
GWP	global warming potential
LT	low temperature
ODP	ozone depletion potential
ORC	organic Rankine cycle
PPTD	pinch point temperature difference
bsfc	brake specific fuel consumption

passenger car under European driving cycle conditions, and revealed that it can reduce the engine's fuel consumption by 8–19% [5]. Mondejar et al. performed a quasi-steady state simulation of an ORC system for a passenger ship, and reported that it could meet around 22% of the total power demand on board [6].

The thermal efficiency of ORC systems strongly depends on the characteristics of its working fluid. It is therefore critical to select a suitable working fluid for a specific application of waste heat recovery [7,8]. Firstly, the critical temperature of the working fluid should be close to the heat source temperature. Braimakis et al. performed a simulation of ORC system with the heat source temperatures in the range from 150 to 300 °C, and reported that the system's exergetic efficiency was strongly affected by the critical temperature of the working fluids [9].

Secondly, the system structure of an ORC can also affect the working fluid selection. Larsen studied subcritical and supercritical ORCs with 109 working fluids, and reported that recuperated ORC systems with hydrocarbons achieved the best efficiencies while wet and isentropic fluids were more suitable for non-recuperated ORC systems [10]. For power generation from a heat source at 150 °C, Le et al. found that R32 and R152a were the best working fluids for the basic and regenerative cycles, respectively [11].

Thirdly, the effect of operating parameters such as evaporation pressure and temperature should also be considered for working fluid selection [12]. Toffolo et al. used a multi-criteria approach, including the pressure and temperature at the turbine inlet, to compare the performance of different working fluids [13]. The selection of working fluids also depends on the design target. For instance, Yang and Yeh investigated an ORC system for waste heat recovery from a diesel engine, and found that their system achieved the optimal economic performance and the highest thermal efficiency with R245fa and R1234ze as working fluid, respectively [14]. In addition, the working fluids for ORC systems on vehicles and ships should be non-toxic, non-flammable, and environmentally friendly.

There are two types of waste heat sources discharged by IC engines, exhaust gases with a temperature above 200 °C and coolants with a temperature in the range 80–120 °C. Shu et al. investigated the performance of an ORC system for recovering heat from an engine's exhaust gases, and found it could reduce the engine's fuel consumption by up to 10% when using cyclohexane as working fluid [15]. Di Battista et al. conducted an experimental study of a regenerative ORC system to recover energy from the exhaust gases of an IVECO F1C diesel engine, and reported that it could improve the overall energy efficiency by 4–5% [16].

It is challenging to use a single ORC system to recover heat energy from both the exhaust gases and coolant of IC engines due to their different temperatures. Song et al. developed an ORC system that uses the coolant of an IC engine to preheat, and subsequently uses its exhaust gas to evaporate the working fluid. The net power output was slightly lower than that of two separate ORC systems but the capital cost of the single-loop system was lower [17]. Kim et al. reported that a single-loop ORC system recovering energy for such application could generate approximately 20% extra power [18]. In an IC engine, apart from its exhaust gases, the coolant also contains a considerable amount of waste heat, however at a much lower temperature. The maximum temperature of the single-loop ORC is usually constrained due to the utilisation of a single working fluid, resulting in higher irreversibility within the evaporator.

To address this challenge, BMW proposed a dual-loop Rankine cycle system which uses water and ethanol as working fluids for the high-temperature (HT) and low-temperature (LT) cycles, respectively [19]. Since then, several studies have been conducted to evaluate the performance of dual-loop organic Rankine cycle (DORC) systems using various working fluids [20–22]. Shu et al. proposed a regenerative DORC and evaluated its performances using water, siloxane, toluene, decane, cyclohexane, and D4 for the high-temperature loop, while using R143a, R125, R218, and R41 for the low-temperature loop [23].

DORC can utilise the waste heat of both the exhaust gases and coolant. Although two expanders are required for a DORC system, the expansion ratio of each is small and thus a higher efficiency can be achieved. So far, some working fluids have been considered for DORC systems due to their good thermodynamic performance, but they are either toxic or not environmental friendly. More efforts are then needed to identify or develop new working fluids for such applications.

Furthermore, there have been growing interests in supercritical ORCs recently, which can potentially achieve better thermodynamic performance than subcritical cycles [24]. Maraver et al. analysed the performance of several optimised subcritical and supercritical ORCs using R134a, R245fa, SES36, n-pentane, MDM, and toluene as working fluids [25]. Glover et al. designed a supercritical single-loop ORC for engine waste heat recovery, and its maximum thermal efficiency could reach 19% [26].

Different working fluid pairs have been considered for dual loop ORC systems by various research groups. BMW used water for the HT loop and ethanol for the LT loop [19]. Wang et al. suggested R245fa and R134a for the HT and LT loops, respectively [20]. Later, Tian et al. studied various working fluids for a regenerative DORC system and found that using toluene for the HT loop and R143a for the LT loop could achieve the highest thermal efficiency [27]. Among these working fluids, R245fa and R134a have low boiling temperatures and are not flammable. However, the GWP of these two fluids are greater than 1000 and thus they are not considered to be environmentally friendly. In this paper, two new environmentally friendly refrigerants, R1233zd and R1234yf, are proposed for the HT and LT loops, respectively.

This paper examines a regenerative supercritical-subcritical DORC for recovering waste heat from both the exhaust gases and coolant of a compressed natural gas (CNG) engine. Unlike most previous studies focusing on the ORC system only, the present research analyses the integrated engine-ORC system. As such, the ORC system is analysed on the basis of real characteristics of waste heat sources of the CNG engine under various operating conditions.

A numerical model is developed to analyse the performance of the proposed dual loop ORC system with four pairs of working fluids. The effects of regeneration and other key operating parameters are also analysed and discussed in detail. The performance of the integrated engine-ORC system is then analysed under real engine operating conditions which were measured beforehand. The obtained results show that the proposed dual loop system could achieve better performance than other ORC systems for similar applications. The potential of fuel saving gained by applying such waste heat recovery system has been evaluated. The research results show that the proposed DORC system can improve the engine's fuel efficiency significantly.

2. The proposed system and its thermodynamic modelling

The proposed regenerative, supercritical-subcritical, dual-loop organic Rankine cycle (DORC) is schematically shown in Fig. 1. The yellow[1] dash-dotted lines represent a regenerative high temperature (HT) loop that recovers waste heat from the exhaust gases. It consists of Reservoir 1, Pump 1, Regenerator 1, Evaporator 1, Turbine 1, and Condenser, which also works as a Preheater for the LT loop. The green dashed lines indicate a regenerative low temperature (LT) loop that recovers energy from the coolant, the condenser of the HT loop, and the exhaust gases. It consists of Reservoir 2, Pump 2, Regenerator 2, the preheater, Evaporator 2, a superheater, Turbine 2, and a condenser. The preheater of the LT loop also works as the condenser of the HT loop.

In this study, the condensation temperature of the HT loop is assumed to be lower than the coolant temperature, so the preheater is installed at the upstream of Evaporator 2 within the low temperature loop. As such, more heat can be extracted from the exhaust gases and transferred to the working fluid in the HT loop. As the thermal efficiency of the supercritical HT loop is much higher than that of the LT loop, this arrangement is beneficial for improving the overall energy recovery efficiency. In addition, Regenerator 1 is employed to recover heat from the superheated vapour exiting from Turbine 1 to heat the subcooled liquid exiting from Pump 1. Regenerator 2 is employed to further improve the thermal efficiency of the LT loop. R1234yf, used in the LT loop, is a dry fluid and thus superheating is normally not required to protect Turbine 2. It is however still beneficial to have a superheater and the benefits are twofold. First, the temperature of the exhaust gases exiting can be further reduced before discharging to the environment so that more waste heat can be recovered. Second, the superheater can raise the temperature of the vapour of R1234yf at the inlet of the Turbine 2, improving the thermal efficiency of the LT loop.

The temperature-entropy diagram of the proposed system (as described in Fig. 1) is shown in Fig. 2. The red and blue domes represent the saturation liquid and vapour lines of R1233zd and R1234yf, respectively. The magenta lines represent the regenerative supercritical HT loop (i.e., HT1–HT6) using R1233zd as working fluid, while the green lines denote the regenerative subcritical LT loop (i.e., LT1–LT8) using R1234yf as working fluid. The same numbering sequence has been used in both Figs. 1 and 2 for the convenience of analysis.

Within the HT loop, liquid R1233zd is pumped from Reservoir 1 to Regenerator 1, where it absorbs heat from the high-temperature vapour phase exiting Turbine 1. The corresponding working processes are represented by HT1 → HT2 and HT2 → HT3 as shown in Fig. 2. Liquid R1233zd then enters into Evaporator 1 where it is heated by the exhaust gases and turns into a supercritical state HT4. It then expands within Turbine 1, turns into a superheated state, and then flows into Regenerator 1. The high enthalpy contained in the superheated vapour of R1233zd at state HT5 justifies the need for Regenerator 1.

Within the LT loop, Pump 2 delivers the working fluid R1234yf from Reservoir 2 to Regenerator 2. The heated subcooled liquid at state LT3 then enters the preheater, where the liquid R1234yf turns into a two-phase state LT4. The coolant from the engine jacket heats and evaporates it into a superheated state LT5 in Evaporator 2. Subsequently, the vapour is further heated to a superheated state LT6 by the exhaust gases in the superheater. The superheated vapour of R1234yf expands in Turbine 2 to produce mechanical work. The low-pressure superheated vapour at state LT7 is then cooled to state LT8 in Regenerator 2. It is finally condensed and turned into a saturated liquid (i.e., state LT1) in the condenser.

Based on the thermodynamic principles described above, a mathematic model is then employed to simulate the proposed system. The detailed model is presented in Appendix A. In this model, the ORC cycles are assumed to operate at steady-state conditions. The pressure and heat losses along all pipes and heat exchangers are assumed to be negligible. The key parameters for the thermodynamic model are listed in Table 1. For all simulations, the temperature and pressure at the inlet of the turbine of the HT loop are specified in a range of interest.

[1] For interpretation of color in Figs. 1–3, 5 and 12, the reader is referred to the web version of this article.

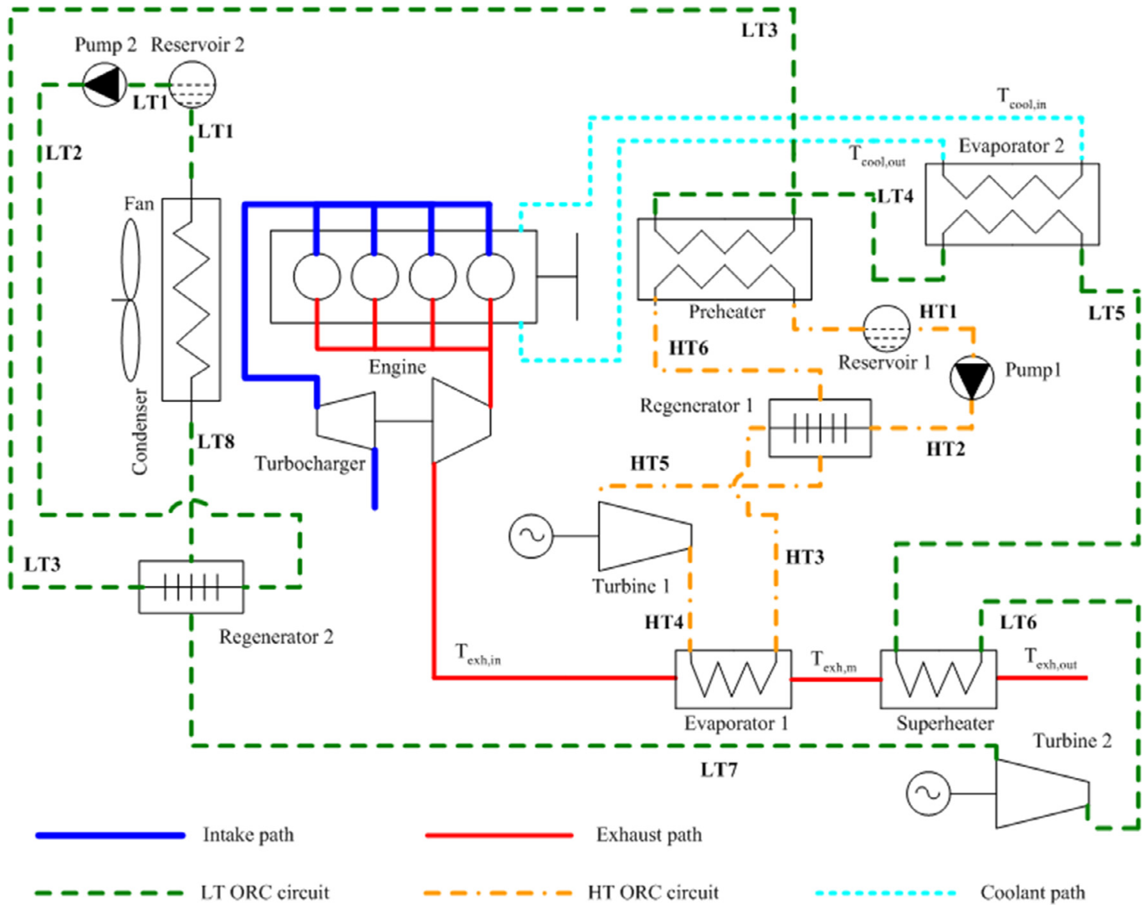

Fig. 1. Schematic of a regenerative supercritical-subcritical DORC for waste heat recovery from IC engines.

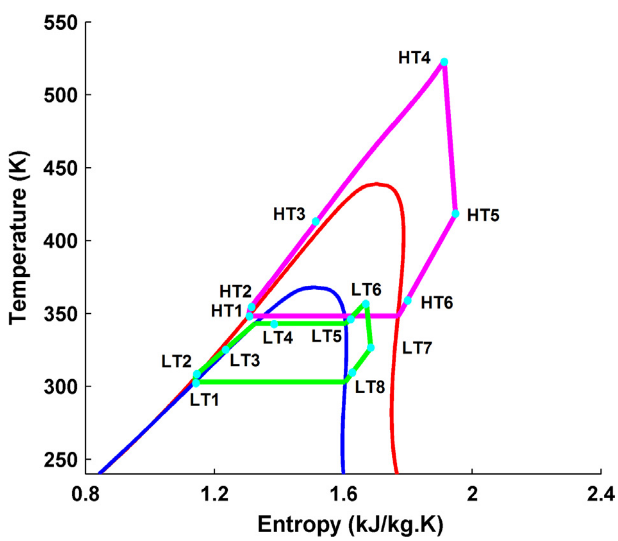

Fig. 2. Working principle of the regenerative supercritical-subcritical DORC.

Table 1
Input parameters for the thermodynamic model.

Parameter	Unit
Maximum turbine inlet pressure of the HT loop	10 MPa
Condensation temperature of the HT loop	75 °C
PPTD of Evaporator 1	20 °C
PPTD of Regenerator 1	5 °C
PPTD of the preheater	5 °C
PPTD of Evaporator 2	5 °C
PPTD of the superheater	20 °C
PPTD of Regenerator 2	5 °C
PPTD of the condenser	9 °C
Isentropic efficiency of Turbines 1 and 2	0.75
Isentropic efficiency of Pumps 1 and 2	0.80

Table 2
Specifications of the CNG engine.

Item	Parameter	Unit
Displacement	8.9	L
Bore × stroke	114 × 144	mm
Cylinder number	6	–
Rated power	210	kW
Rated speed	2200	r/min
Max. torque	1150	N m
Speed at max. torque	1400	r/min

3. Characteristics of waste heat sources of a CNG engine

The proposed DORC system is developed for energy recovery from the waste heat sources of a compressed natural gas (CNG) engine that is widely used on city buses in China. Differing from diesel/petrol engines, CNG engine is fuelled with natural gas and thus has several advantages such as low emissions and high efficiency. It is therefore suitable for operation in densely populated cities [28] where air pollution in becoming a major issue. The CNG engine considered in this research is the same as that in Ref. [29], and its technical specifications are listed in Table 2. The measured engine performance and characteristics of its waste heat sources are shown in Fig. 3.

The engine performance map is shown in Fig. 3a, where the red dashed lines represent the contours of the power output (kW), the solid lines are the contours of brake specific fuel consumption (bsfc, g/kW·h). The corresponding map for the effective thermal efficiency is shown in Fig. 3b. The maximum thermal efficiency is about 41% when the engine operated with 100% load at an engine speed of 1400 RPM. The measured temperature of the exhaust gases is mapped in Fig. 3c. The temperature of the exhaust gases is above 500 °C in all operation regions of this engine, and it increases as the engine load and speed increase. The map of mass flow rate of the exhaust gases is given in Fig. 3d. It increases from 0.02 to 0.30 kg/s as the engine power increases. The mass flow

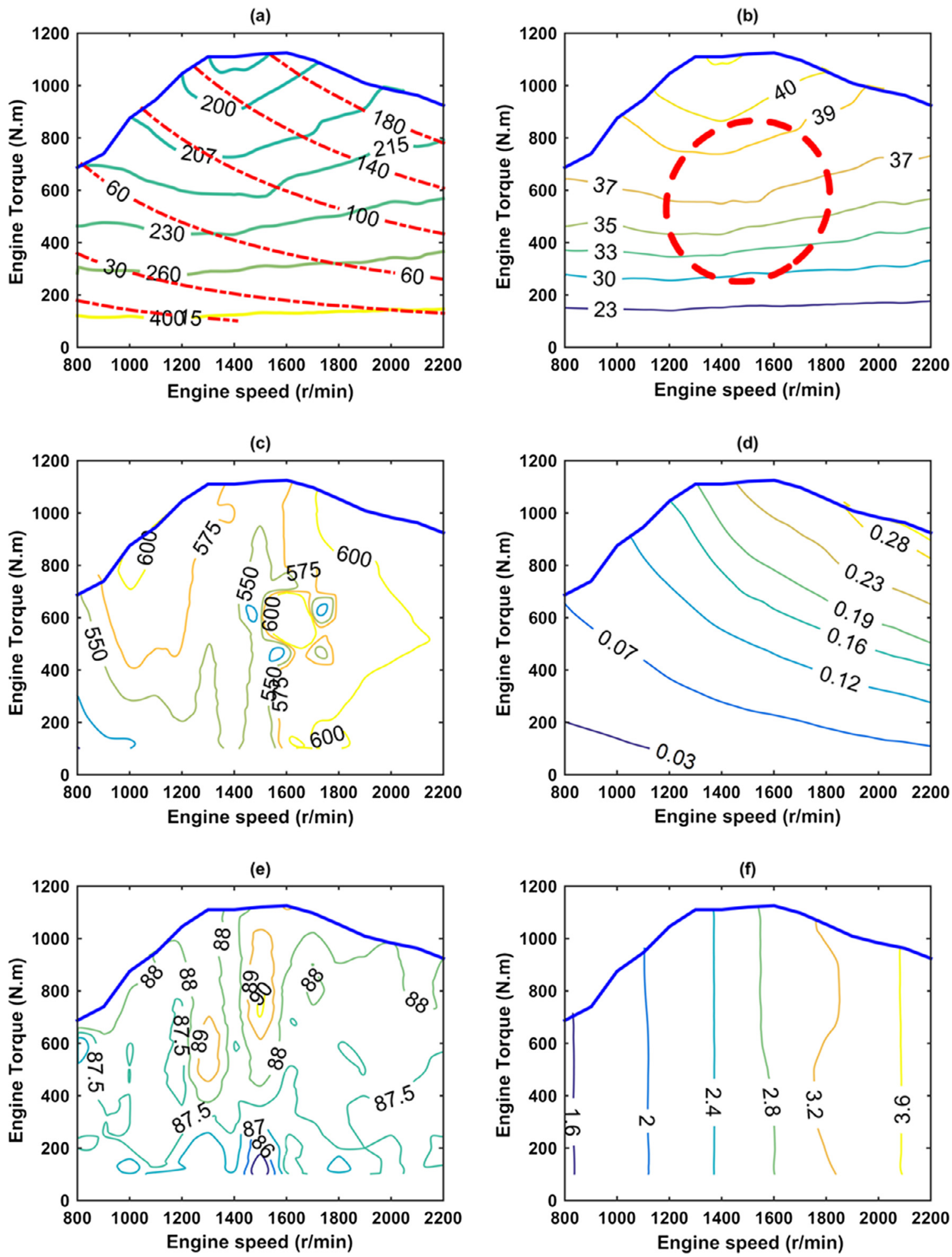

Fig. 3. Measured data of a CNG engine: (a) the power output (kW) and bsfc (g/kW·h); (b) the effective thermal efficiency (%); (c) the temperature of its exhaust gases (°C); (d) the mass flow of its exhaust gases (kg/s); (e) the temperature of its coolant (°C); (f) the mass flow of its coolant (kg/s).

rates of the intake air and the fuel increase accordingly. The map of the coolant temperature at the outlet of the engine cooling jacket is shown in Fig. 3e. The coolant temperature varies in the range from 85 to 90 °C in all operation regions. The map of the coolant mass flow rate is shown in Fig. 3f. The coolant mass flow increases from 1.6 to 3.8 kg/s as the engine speed increases from 800 to 2200 r/min. Since the coolant pump is driven by the engine crankshaft via a pair of gears, the mass flow rate of the coolant pump is proportional to the engine speed.

4. Performance of the supercritical HT ORC loop

In addition to the proposed R1233zd and R1234yf, the simulations have also used other three pairs of working fluids for comparison, including R245fa/R134a, toluene/R143a, and water/ethanol. A comparison of the properties of these working fluids is summarised in Table 3. The corresponding saturated liquid and gas curves are plotted in Fig. 4. Water and ethanol are wet working fluids, while the others are dry working fluids. The critical temperatures of water, toluene, and ethanol are much higher than that of the others.

To compare the thermodynamic performance of the proposed DORC system using these four pairs of working fluids, the thermal efficiency of the supercritical HT loop is firstly computed based on the developed mathematical model. The ambient temperature is assumed to be 5 °C. Fig. 5 shows the calculated thermal efficiency of the supercritical HT loop as a function of the turbine inlet pressure and temperature.

The turbine inlet pressure is set in the range of 4–10 MPa when R1233zd, R245fa, and water are used as the working fluids. As the critical pressure of toluene is 4.126 MPa, the turbine inlet pressure is set in the range of 4.2–10 MPa when it is used as working fluid. Therefore, the HT loop operates on a supercritical cycle when using R1233zd, R245fa, or toluene as its working fluid. However, the critical pressure of water is 22.064 MPa, the HT loop is therefore a subcritical cycle when it uses water as working fluid. In addition, the turbine inlet temperature for the working fluids of R1233zd and R245fa is kept below 300 °C. The maximum turbine inlet temperatures of toluene and water are set to 460 °C and 500 °C, respectively.

Fig. 5a shows the thermal efficiency of the system with R1233zd as working fluid. The upper surface represents the thermal efficiency of the regenerative ORC as a function of the temperature and pressure at the inlet of the turbine while the lower surface shows results of a basic ORC without regeneration. Similarly, the calculated thermal efficiency of the system using R245fa, toluene, and water as working fluids are shown in Fig. 5b through d.

It can be seen that the system's thermal efficiency strongly depends on the temperature at the inlet of the turbine. The higher the temperature, the higher the thermal efficiency. The results of Fig. 5 also indicate that regeneration can significantly improve the system's thermal efficiency when using R1233zd, R245fa, and toluene as the working fluid. However, if the turbine inlet temperature is too low, the thermal efficiency of the regenerative ORC is equal to that of the basic ORC. Under these conditions, a regenerator is not desirable because the turbine outlet temperature is too low for recuperation. The difference in thermal efficiency between the regenerative and the basic ORCs increases as the turbine inlet temperature increases. When the turbine inlet temperature is 300 °C, the thermal efficiency of the regenerative ORC is about 1.5 times that of the basic ORC when the working fluid is R1233zd. For the ORC using toluene, the thermal efficiency of the regenerative ORC is always greater than that of the basic ORC. However, when water is used as the working fluid, the thermal efficiency of the regenerative ORC is almost the same as the basic ORC as shown in Fig. 5d. This can be attributed to the fact that water is a wet working fluid, and thus the degree of superheat of the steam at the turbine outlet is too low for heat recuperation.

In order to further understand the results presented in Fig. 5, several cases using R1233zd and R245fa as working fluids for a given turbine inlet pressure have been extracted and shown in Fig. 6. The solid lines A1 and B1 represent the regenerative ORC using R1233zd and R245fa, respectively. Dashed lines A2 and B2 denote the basic ORC using R1233zd and R245fa, respectively. When the turbine inlet pressure is kept as 6 MPa, the thermal efficiencies are then calculated when the turbine inlet temperature varies. The obtained results are shown in Fig. 6a. Similarly, the calculated results when the turbine inlet pressures are kept as 8 and 10 MPa are given in Fig. 6b and c, respectively. It can be clearly seen that both the supercritical cycles have almost the same thermal efficiency as their basic counterparts when the turbine inlet temperature is relatively low (e.g., below 200 °C in Fig. 6b). However, as temperature increases, the benefit of using supercritical cycle becomes significant. The higher the turbine inlet temperature, the larger the difference of thermal efficiency.

The maximum thermal efficiencies shown as the red lines in Fig. 5 as a function of the turbine inlet pressure are shown in Fig. 6d. It can be seen that the turbine inlet pressure has a very small effect on the thermal efficiency of both the regenerative and basic ORCs. Their thermal efficiencies only increase slightly with the increase of the turbine inlet pressure.

It can be seen from Fig. 6 that the turbine inlet temperature of the regenerative ORC has to be higher enough to benefit from the recuperation, and that the threshold temperature depends on the working fluid and turbine inlet pressure. Fig. 7 shows the threshold turbine inlet temperatures as a function of the turbine inlet pressure for R1233zd and R245fa cycles. The threshold temperature increases as the turbine inlet pressure increases, and it is higher for R1233zd cycle than R245fa cycle.

Similarly, the results for toluene and water cycles are shown in Fig. 8, where C1 and D1 represent the regenerative ORCs with toluene and water as working fluid, respectively, while C2 and D2 are the basic ORCs using toluene and water as working fluid,

Table 3
Properties of the working fluids.

Working fluid	Molecular mass (kg/kmol)	Normal boiling point (K)	Critical pressure (MPa)	Critical temperature (K)	ASHRAE 34 safety group	ODP	GWP
R1233zd	130.5	291.47	3.5709	438.75	A1	0	5
R245fa	134.05	288.05	3.639	427.2	B1	0	1030
Toluene	92.138	383.75	4.1263	591.75	n/a	n/a	n/a
Water	18.015	373.12	22.064	647.1	n/a	n/a	n/a
R1234yf	114.04	243.7	3.3822	367.85	A2L	0	4
R134a	102.03	247.08	4.059	374.21	A1	0	1430
R143a	84.041	225.91	3.761	345.86	A2L	0	4427
Ethanol	46.068	351.57	6.268	514.71	n/a	n/a	n/a

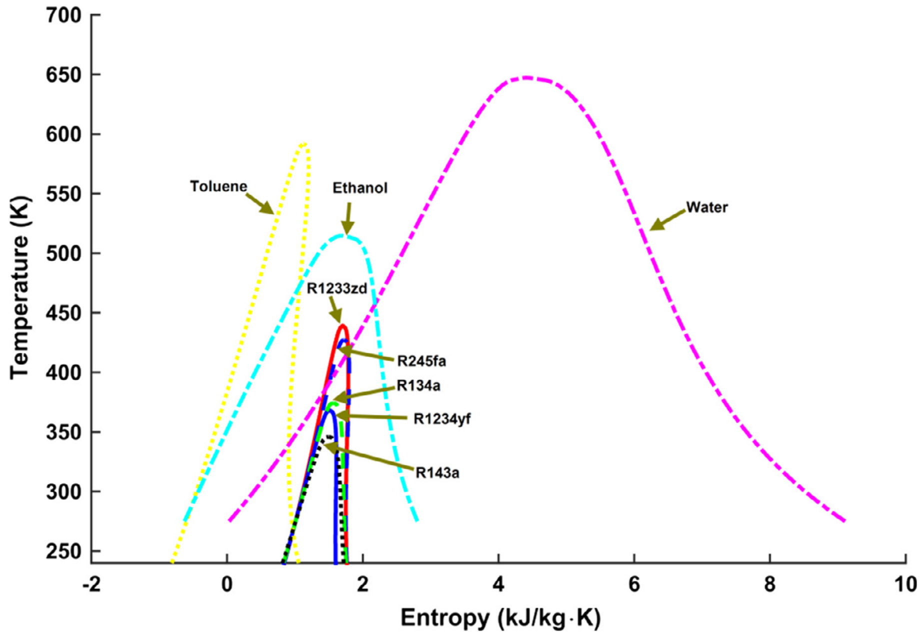

Fig. 4. The saturation lines of the different tested working fluids on a temperature-entropy diagram.

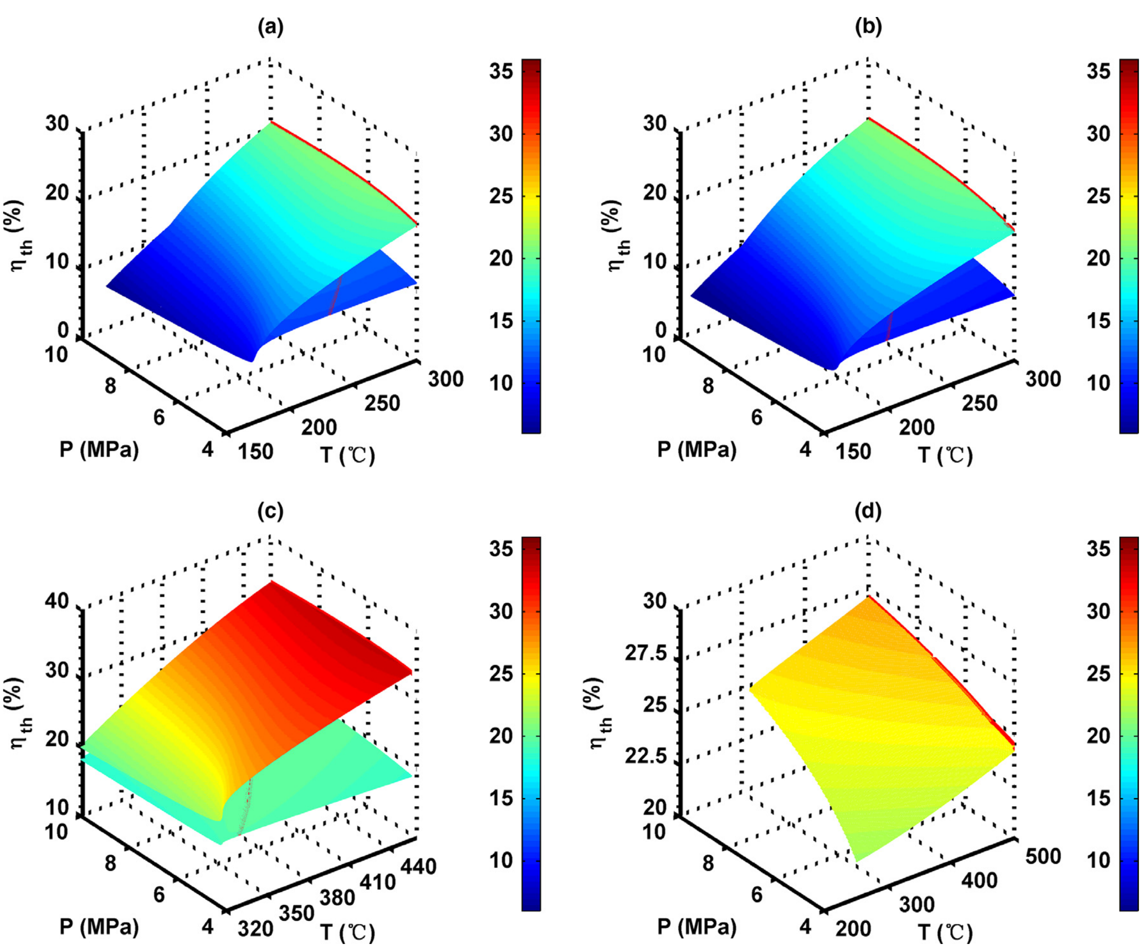

Fig. 5. Performance comparison of the supercritical HT loop using different working fluids: (a) R1233zd; (b) R245fa; (c) toluene; (d) water.

respectively. It can be seen that the required turbine inlet temperatures of toluene and water cycles are much higher than R1233zd and R245fa cycles. For the toluene and water cycles, increasing the turbine inlet pressure can also only improve the thermal efficiency very little. Therefore, for a regenerative supercritical ORC, the turbine inlet pressure can be set to a relatively low level, while

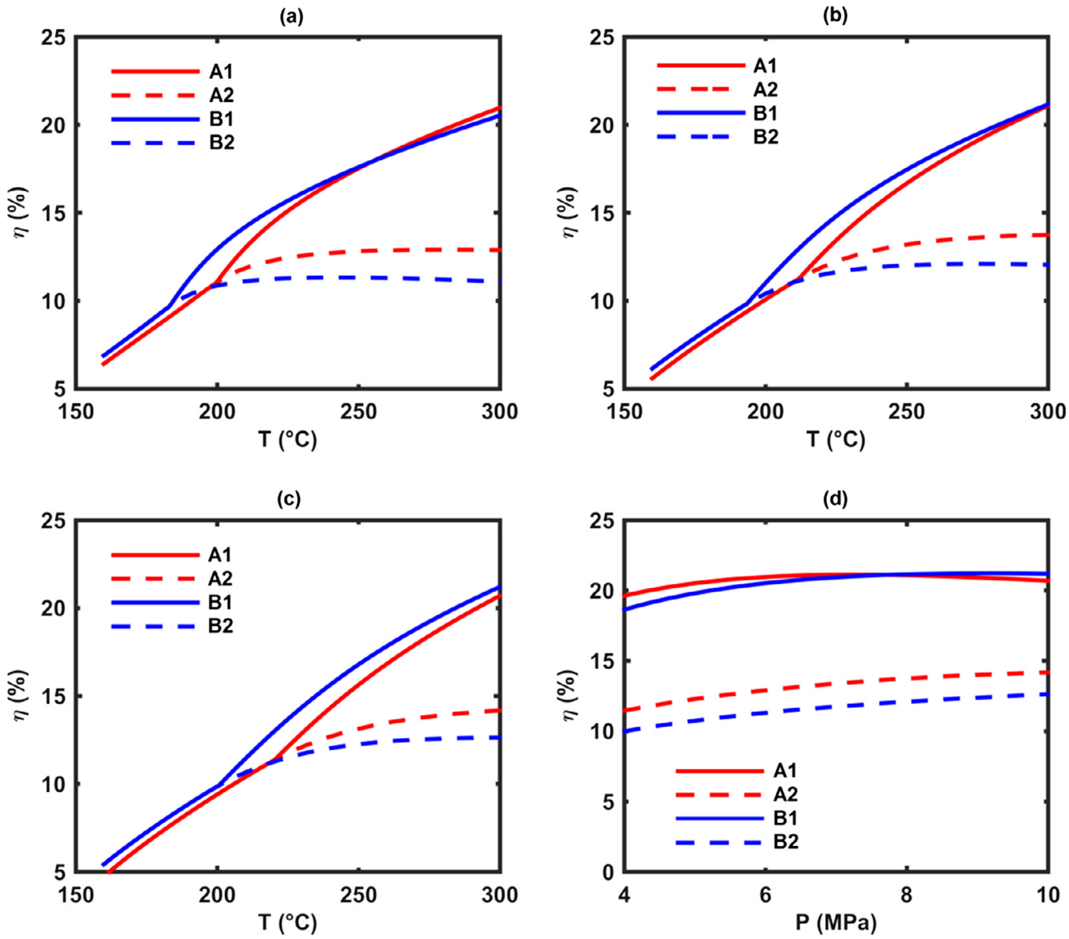

Fig. 6. Effects of the turbine inlet pressure and temperature on the performance of the supercritical ORC based on R1233zd and R245fa: (a) P_{HT4} = 6 MPa; (b) P_{HT4} = 8 MPa; (c) P_{HT4} = 10 MPa; (d) the maximum thermal efficiency as a function of P_{HT4}. (A1: regenerative ORC with R1233zd; A2: nonregenerative ORC with R1233zd; B1: regenerative ORC with R245fa; B2: nonregenerative ORC with R245fa.)

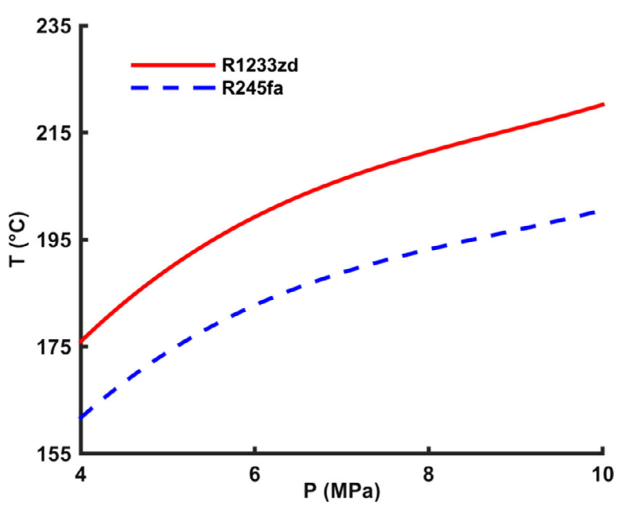

Fig. 7. The threshold temperatures as a function of the turbine inlet pressure of the regenerative supercritical ORC based on R1233zd and R245fa.

the thermal efficiency of the cycle can be then improved by increasing the turbine inlet temperature. For the Rankine cycle using water as working fluid, increasing the turbine inlet temperature can only marginally improve its thermal efficiency. More importantly, to make sure no liquid drops emerge at the turbine outlet when water is used, the turbine inlet temperature has to be higher than a certain value, which is shown as a function of the turbine inlet pressure in Fig. 9.

As discussed above, unlike most of previous studies which analysed the effect of turbine inlet temperature and pressure on the cycle performance separately, this research investigates the effects of recuperation, turbine inlet pressure and temperature, and working fluids together. As such, we can gain a comprehensive understanding of the interactions between these aspects. It is found that regeneration is not desirable for wet working fluids, while it is beneficial for dry working fluids when the turbine inlet temperature and pressure must be high enough so that the superheated vapour exiting the turbine still contains considerable heat energy.

5. Working fluid selection for DORC

In this section, the thermodynamic performances of the proposed DORC using the four different pairs of working fluids are analysed. The CNG engine usually operates at low to middle speed and torque for bus applications (please see the red dashed line circle in Fig. 3b). Therefore, an operation point at an engine speed of 1600 RPM and with a torque of 600 N m is selected as a case study. Based on the mathematical model as described in Appendix A, for each pair of working fluids, the thermodynamic performances of the HT and LT loops are calculated and listed in Tables 4 and 5. The turbine inlet pressure of the HT loop is set as 6 MPa. The turbine inlet temperature of the HT loop for R1233zd, R245fa, and

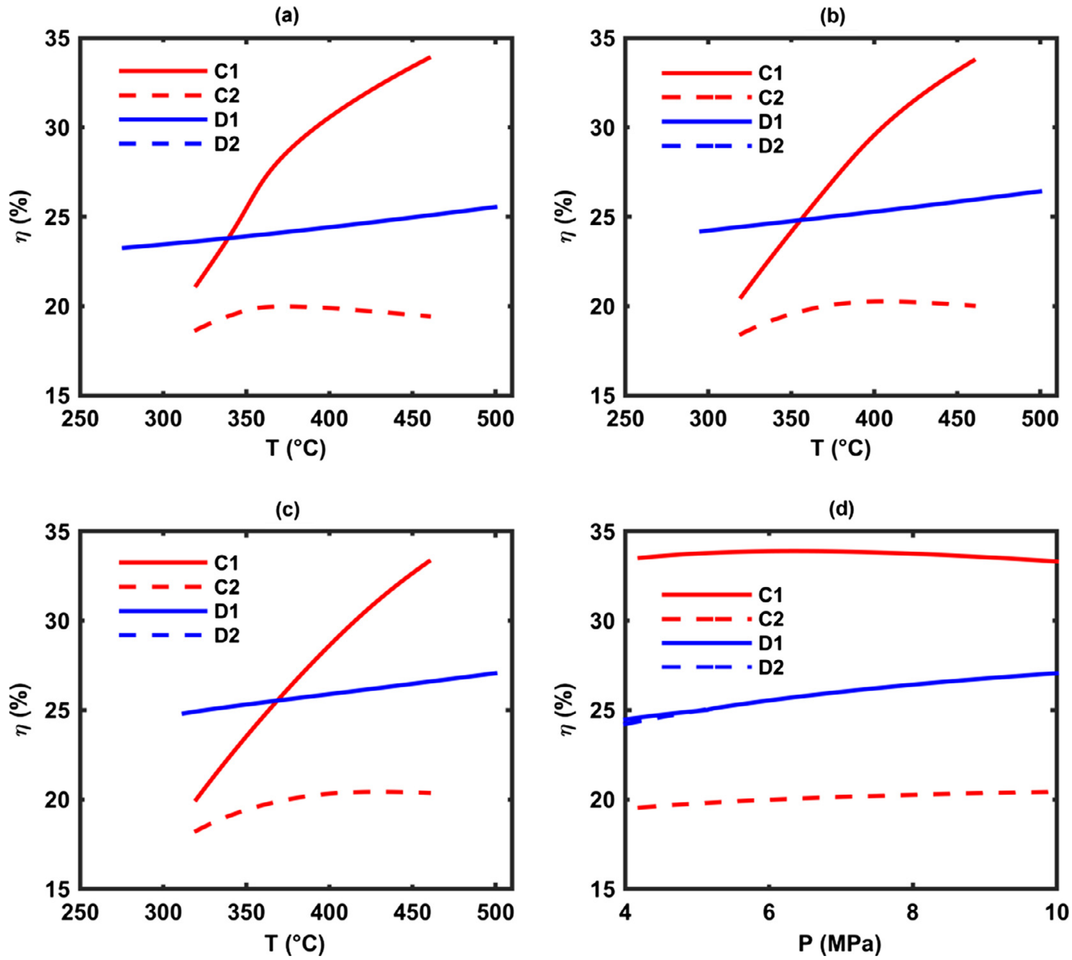

Fig. 8. Effects of the turbine inlet pressure and temperature on the performance of the supercritical ORC based on toluene and water: (a) P_{HT4} = 6 MPa; (b) P_{HT4} = 8 MPa; (c) P_{HT4} = 10 MPa; (d) the maximum thermal efficiency as a function of P_{HT4}. (C1: regenerative ORC with toluene; C2: nonregenerative ORC with toluene; D1: regenerative ORC with water; D2: nonregenerative ORC with water.)

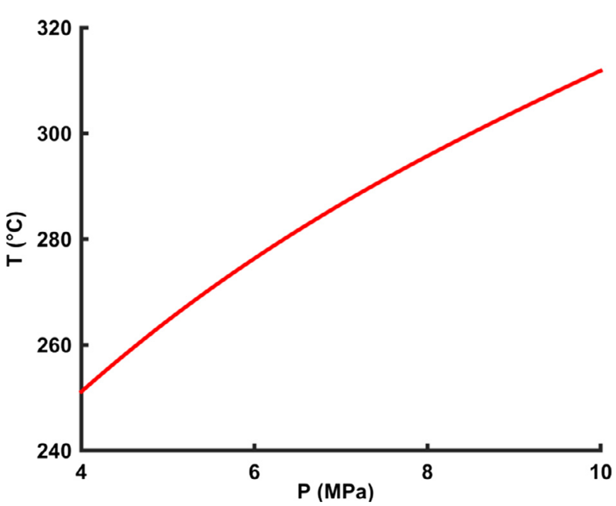

Fig. 9. The threshold temperature as a function of the turbine inlet pressure of the HT loop using water as working fluid.

water cycles are set as 300 °C, while it is set as 320 °C for toluene cycle.

To compare the performance of the turbines with different working fluids, two important indices for a turbine expander, i.e., volumetric flow ratio (VFR) and size parameter (SP), are adopted [30]. They are defined as

$$VFR = V_{out}/V_{in}, \tag{1}$$

and

$$SP = \frac{\sqrt{V_{out}}}{\Delta h_{is}^{0.25}}, \tag{2}$$

where V_{out} and V_{in} are the volumetric flow rates at the outlet and inlet of a turbine, Δh_{is} is the enthalpy drop in the turbine along the isentropic expansion. The VFR determines the number of turbine stages. A smaller value of VFR means that fewer stages are required, leading to higher isentropic turbine efficiency. Generally, a high isentropic efficiency can be obtained if the VFR is less than 100 (the VFR of a single stage is less than 10) [30,31]. The SP is an indicator of the relative size of the turbine. A large SP indicates that the outer diameter of the turbine is larger, leading to higher cost.

The designed DORC has several heat exchangers. Normally, the size and cost of a heat exchanger can be estimated by its *UA* value which is the multiplication of the heat transfer coefficient *U* and the heat transfer area *A*. A higher *UA* means that a larger size and thus more expensive heat exchanger is required. The *UA* is determined by

$$UA = \frac{Q}{\Delta T_{lm}}, \tag{3}$$

Table 4
Performance comparison of the HT loop using different working fluids.

Fluids	m_{HT} (kg/s)	W_{p1} (kW)	W_{t1} (kW)	$W_{n,HT}$ (kW)	SP_{t1} (cm)	VFR_{t1}	UA_{e1} (W/K)	UA_{r1} (W/K)	UA_{pre} (W/K)	$\eta_{th,HT}$ (%)
R1233zd	0.3315	1.97	17.13	15.16	0.8125	10.89	729	2441	2309	21.16
R245fa	0.3352	1.85	16.39	14.54	0.7638	8.94	717	2756	2101	20.65
Toluene	0.1658	1.51	19.29	17.78	2.164	537	890	1222	2437	21.42
Water	0.0354	0.27	21.56	21.29	1.172	96.5	924	–	3141	23.45

Table 5
Performance comparison of the LT loop using different working fluids.

Fluids	m_{LT} (kg/s)	W_{p2} (kW)	W_{t2} (kW)	$W_{n,LT}$ (kW)	SP_{t2} (cm)	VFR_{t2}	UA_{e2} (W/K)	UA_s (W/K)	UA_{r2} (W/K)	UA_c (W/K)	$\eta_{th,LT}$ (%)
R1234yf	0.7473	1.27	15.82	14.55	1.364	4.44	4569	284	2489	9610	10.90
R134a	0.6218	1.02	15.50	14.48	1.277	4.56	4020	281	1491	9705	10.80
R143a	0.6520	2.16	15.25	13.09	0.988	4.14	8120	192	1390	9134	10.00
Ethanol	0.1275	0.014	14.55	14.54	6.147	13.6	4834	–	–	12,081	11.25

where Q is the heat transfer and ΔT_{lm} is the logarithmic mean temperature difference. For a countercurrent heat exchanger, ΔT_{lm} can be expressed by

$$\Delta T_{lm} = \frac{\Delta T_1 - \Delta T_2}{\ln\left(\frac{\Delta T_1}{\Delta T_2}\right)}, \tag{4}$$

where ΔT_1 are the maximum temperature differences at both ends of the heat exchanger, and ΔT_2 is the minimum temperature difference.

The results of the HT loop are shown in Table 4. The mass flow rates of R1233zd and R245fa are large, while the mass flow rate of water is much smaller. The net power output of water cycle is the highest, followed by toluene, R1233zd, and R245fa cycles. However, the SP and VFR values of R1233zd and R245fa cycles are much smaller than that for the toluene and water cycles. Therefore, a turbine with 2–3 stages will be enough for the HT loop using R1233zd or R245fa as working fluids. However, more stages are required for the cycles using toluene or water as working fluids.

The UA values of Evaporator 1 for different working fluids are close, and they are significantly less than those of Regenerator 1 and the preheater. This can be attributed to the larger logarithmic mean temperature difference within Evaporator 1. For the HT loop, the net power output and the thermal efficiency of R1233zd and R245fa cycles are slightly less than those of water and toluene cycles. However, the efficiency of Turbine 1 for R1233zd and R245fa cycles is higher and thus cheaper than those for the toluene and water cycles.

Table 5 shows the simulation results of the LT loop using different working fluids. The largest mass flow rate appears in R1234yf cycle, while the lowest mass flow rate is found in ethanol cycle. The net power of R1234yf and ethanol cycles is higher than R134a and R143a cycles. The SP and VFR of ethanol cycle are much higher than other cycles. The UA values of Evaporator 2 of R143a cycle is large, and also for the condenser of the ethanol cycle. Their thermal efficiencies are very close to each other. However, the total UA values for R1234yf and R134a systems are much less than ethanol and R143a systems because the heat transfer within their condenser is significantly reduced due to Regenerator 2.

In summary, the thermal efficiency of the DORC using water and ethanol is higher than other three cycles, and no regeneration is required. However, the size of the turbines and heat exchangers are larger, and thus more expensive than other three cycles. The DORC systems using R1233zd/R1234yf and R245fa/R134a as working fluids are smaller and thus cheaper than systems using the other two pairs of working fluids. The thermal efficiency of the DORC system based on R1233zd and R1234yf is slightly higher than that based on R245fa and R134a.

According to our simulations, the temperature of exhaust gases has to be higher than 350 °C for the DORC systems using water/ethanol or toluene/R143a as working fluids. In fact, the exhaust gas temperature of diesel or petrol engines is usually in the range of 200–400 °C under city driving conditions. For the regenerative DORC systems based on R1233zd/R1234yf or R245fa/R134a, the turbine inlet temperature of the HT loop can be less than 200 °C (see Fig. 7), so they are more suitable for waste heat recovery from IC engines with relatively low exhaust gas temperature.

Furthermore, toluene is toxic, while ethanol is flammable. The GWP of R245fa, R134a, and R143a are greater than 1000. Therefore, from the viewpoint of safety and environmental protection, they are considered to be not suitable for waste heat recovery from vehicular IC engines. The thermo-physical properties of R1233zd and R1234yf are very close to those of R245fa and R134a, respectively. However, the toxicity and GWP of R1233zd and R1234yf are much lower than R245fa and R134a. Therefore, R1233zd and R1234yf are considered to be the most suitable working fluids for the proposed DORC system.

6. Performance of the combined engine-DORC system

6.1. Performance with constant turbine efficiencies

As concluded in the above, R1233zd and R1234yf are the most suitable working fluids for the proposed regenerative supercritical-subcritical DORC. In this section, we will continue to analyse the performance of the proposed DORC system based on this pair of working fluids under a variety of operating conditions. The mathematical model used in for these simulations is presented in

Table 6
Thermodynamic properties of the regenerative supercritical-subcritical DORC with R1233zd and R1234yf as working fluids.

State no.	Pressure (MPa)	Temperature (K)	Enthalpy (kJ/kg)	Entropy (kJ/kg·K)
HT1	0.581	348.15	294.81	1.305
HT2	6.0	352.26	300.75	1.308
HT3	6.0	447.81	439.58	1.655
HT4	6.0	573.15	655.68	2.086
HT5	0.581	495.21	604.01	2.122
HT6	0.581	357.26	465.18	1.794
LT1	0.510	288.15	219.80	1.070
LT2	2.045	289.29	221.50	1.071
LT3	2.045	309.20	248.95	1.163
LT4	2.045	343.15	324.53	1.391
LT5	2.045	346.72	404.41	1.624
LT6	2.045	363.15	427.57	1.689
LT7	0.510	321.85	406.39	1.711
LT8	0.510	294.29	378.94	1.622

Appendix A. The thermodynamic properties for the states of the DORC are given in Table 6. The turbine inlet pressure and temperature of the supercritical HT loop are set to 6 MPa and 300 °C, respectively. Both the condensation pressures of the HT and LT loops are higher than 5 bar, which can prevent air leaking into the system. The isentropic efficiencies of the two turbines are given as 0.75 [32]. The fuel efficiency improvement of the CNG engine is then evaluated after the proposed ODRC waste heat recovery system is introduced.

Fig. 10 shows the performance maps of the DORC system over the entire operating region of the tested CNG engine. The net power output of the HT and LT loops is given in Fig. 10a and b, respectively. As expected, they increase as the engine's power increases. For a given operation point, the net power output of

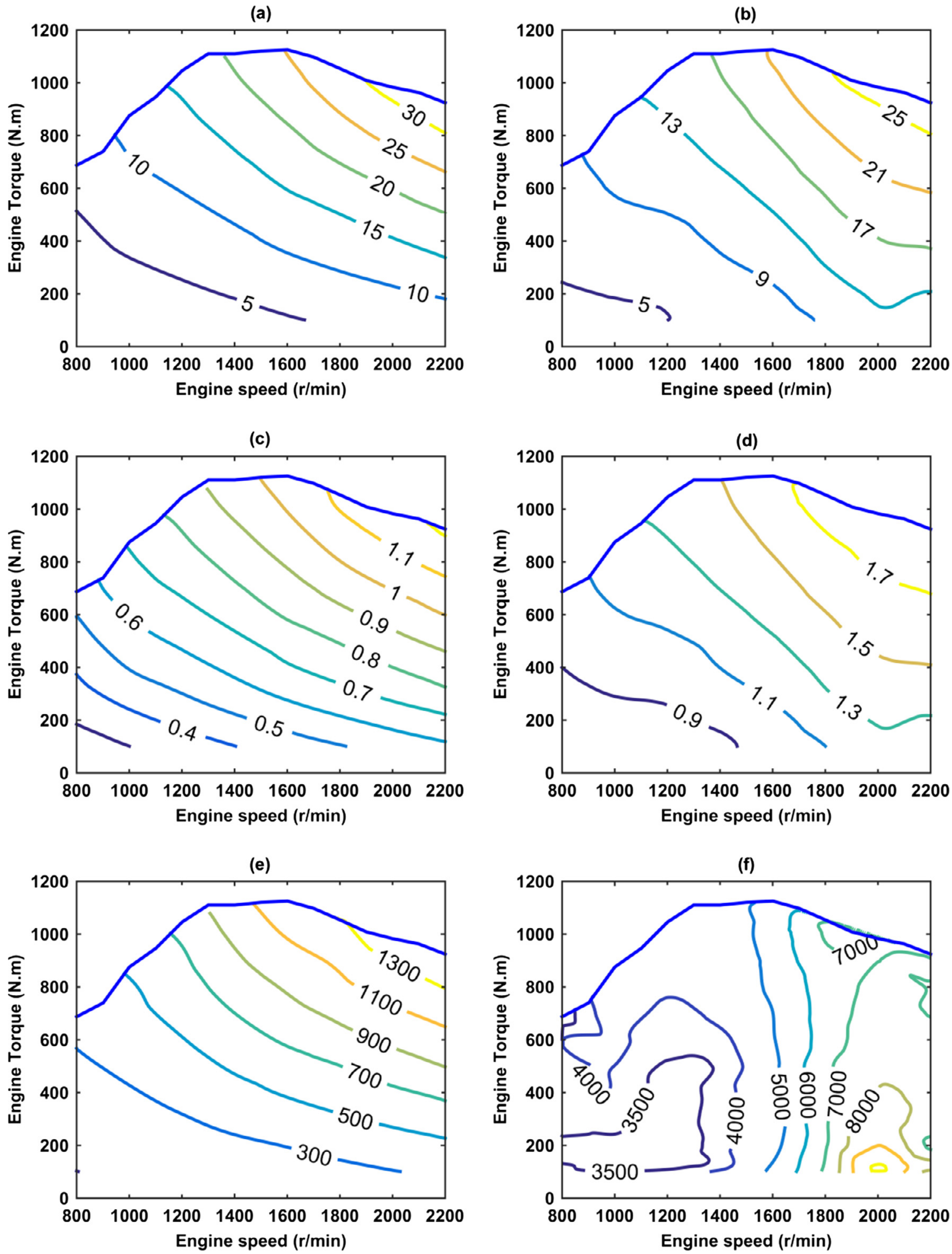

Fig. 10. Performance maps of combined engine-DORC system: (a) the net power output of the HT loop (kW); (b) the net power output of the LT loop (kW); (c) the SP of Turbine 1 (cm); (d) the SP of Turbine 2 (cm); (e) the UA of Evaporator 1 (W/K); (f) the UA of Evaporator 2 (W/K).

the HT loop is slightly higher than that of the LT loop. Although the heat input to the HT loop is less than the LT loop, the thermal efficiency of the HT loop (i.e., a supercritical cycle) has higher thermal efficiency than that of the LT loop.

The size parameters (SP) of the HT and LT loops are calculated and shown in Fig. 10c and d when the engine speed and torque vary. The SP of Turbine 1 (or Turbine 2) increases from 0.3 to 1.1 (or from 0.9 to 1.8) as the engine power increases in the tested range. The SP varying in such large range makes it difficult to design turbines that can operate efficiently over the engine's entire working region. In practice, a CNG engine of a bus mainly works at the red circle zone as shown in Fig. 3b. The corresponding SP values for Turbines 1 and 2 are then narrowed down to 0.6–0.8 and 1.1–1.3, respectively.

The UA of Evaporator 1 is shown in Fig. 10e, which increases from 300 to 1300 W/K as the engine power increases. Similarly, the map of the UA value for Evaporator 2 is shown in Fig. 10f. The UA of Evaporator 2 increases from 3500 to 8000 W/K as the engine speed increases. Because the engine speed for most of the city driving conditions is less than 1800 r/min, the UA value of Evaporator 2 can be selected in the range of 4000–5000 W/K.

The map of the net power of the DORC is given in Fig. 11a. Compared with the power map of the original engine as shown in Fig. 3a, the relative improvement of the net power output is in the range of 23–88%. The relative improvement of the net power output compared with the original engine is defined as

$$\psi_{power,rel} = \frac{\dot{W}_{n,HT} + \dot{W}_{n,LT}}{\dot{W}_{n,eng}} \times 100\% \tag{5}$$

The brake specific fuel consumption (bsfc) of the combined system is shown in Fig. 11b. Compared with the original CNG engine, the bsfc of the combined system can be decreased by about 40 g/kW·h over the engine's entire working region. The effective thermal efficiency of the combined engine-DORC system is shown in Fig. 11c. The absolute improvement of fuel efficiency is given in Fig. 11d. The absolute improvement of the thermal efficiency is defined as

$$\psi_{th,abs} = \eta_{th,comb} - \eta_{th,eng}. \tag{6}$$

The thermal efficiency can be improved by an absolute value of 10–14% under the tested conditions.

The U.S. Department of Energy has set up a SuperTruck program and the Cummins Company planned to increase the fuel efficiency of a class 8 heavy-duty truck by 5% via engine waste heat recovery [33]. According to the results of this research, using the designed regenerative supercritical-subcritical DORC system could potentially achieve the threshold value.

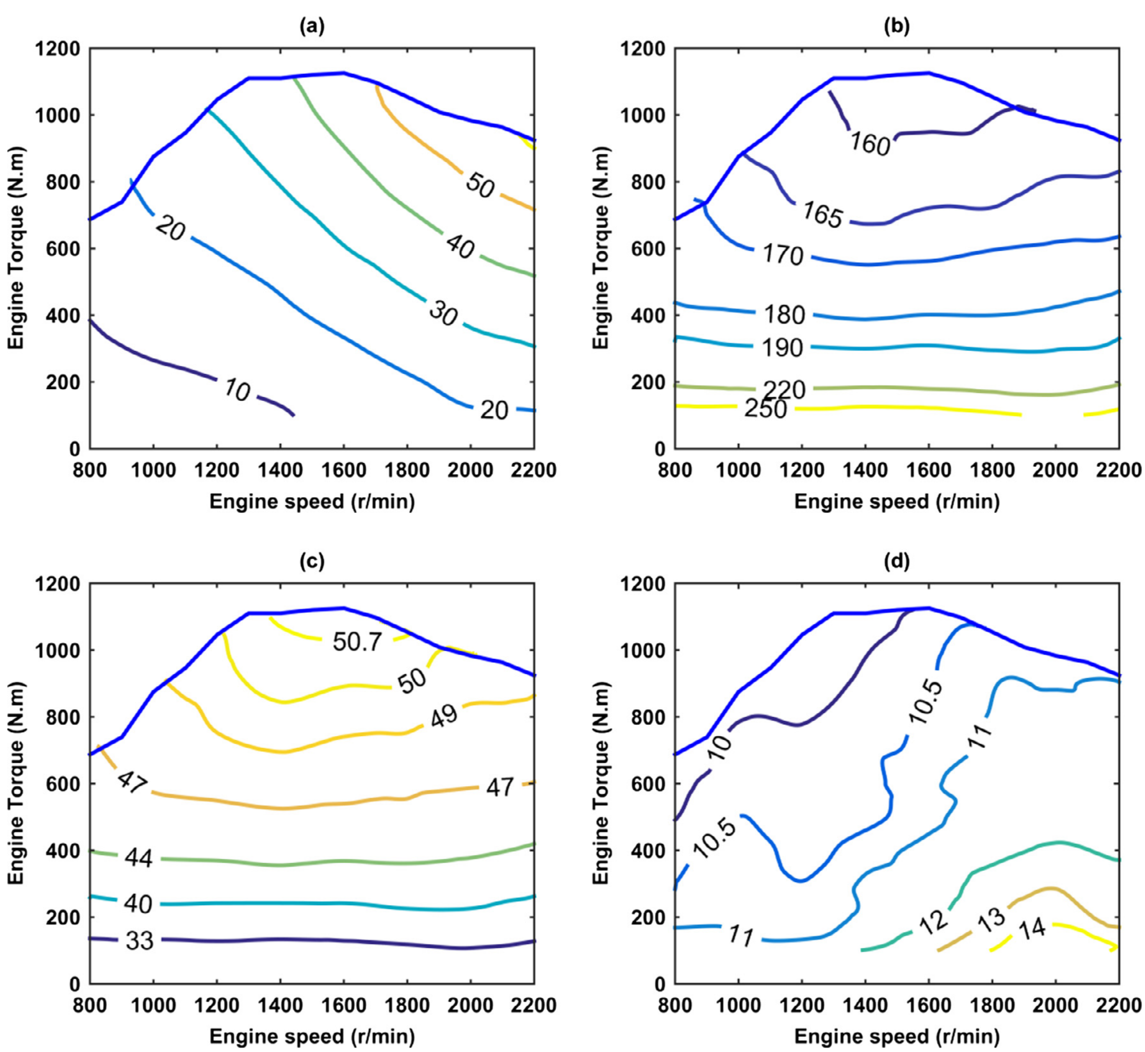

Fig. 11. Performance of the combined engine-DORC system with an ambient temperature of 5 °C: (a) the net power output of the DORC (kW); (b) the bsfc of the combined system (g/kW·h); (c) the effective thermal efficiency of the combined system (%); (d) the absolute improvement of the effective thermal efficiency (%).

6.2. Performance under off-design conditions

In practice, the sizes of the components of DORC system are determined according to a design point where the CNG engine works. However, for other engine working conditions, the DORC system will operate at an off-design state, as a result the turbine efficiency will be lower than the optimised design value. Normally, a DORC system can be designed based on the working conditions at which the CNG engines operate for most of the time. For a heavy-duty vehicle like a bus in urban areas, the vehicle speed of a typical driving cycle (ECE-EUDC-LOW) is shown in Fig. 12a.

In this study, a bus with a curb weight of 13,800 kg and a fully loaded mass of 17,600 kg is used as an example, the corresponding CNG engine working points under this driving cycle are obtained by Advisor and Matlab. Fig. 12b shows the results of a 20% loaded weight and Fig. 12c is the results when it is fully loaded. In these two figures, the blue points represent urban driving conditions while the red points are for highway conditions. It can be seen that the engine's working points under highway conditions are located in the middle/high speed and high load regions denoted by the magenta ellipses. In contrast, the urban conditions are mainly distributed in the region with an engine speed of 1000–1800 r/min and an engine load of 50–100% represented by the cyan ellipses. Therefore, for a bus driving on highways for most of the time, the design point of the DORC system should be based on the rated engine point shown as Point A in Fig. 12c. However, for a bus running in urban areas, the design point of the DORC should be close to the cyan ellipse (e.g., Point B) in Fig. 12c, where the engine speed is 1400 r/min and the engine load is 100%.

When matching the DORC system with the CNG engine, the two turbines' efficiencies will decrease at the off-design points. The drop of the turbines' efficiencies has a significant effect on the DORC performance. Two-stage axial-inflow turbines are suitable for the proposed DORC system due to their very high expansion ratios.

To obtain the turbine efficiency under off-design conditions, the method presented in [32] is adopted in this study. The isentropic efficiency of the turbine is computed starting from the isentropic efficiency of 0.75 under the optimised design conditions. Two correction factors have been employed. The first correction factor is associated with the variation of u/c_0 due to the variation of the isentropic enthalpy drop under off-design conditions. The second correction factor takes into account the variation of the mass flow rate from the design value.

When Point B is selected as the design point of the DORC system, the results are given in Fig. 13a and b. The map of the net power output of the DORC system is shown in Fig. 13a. Fig. 13b shows the improvement of the thermal efficiency. Compared with that with constant turbine efficiency shown in Fig. 11a, the net power output of the DORC system drops slightly in the middle-speed and high-load region. However, in the low-speed/small-load and high-speed/large-load regions, the net power output decreases significantly. Nevertheless, the improvement of the thermal efficiency still can be above 8% even under urban driving conditions.

When Point A is selected as the design point, the results are obtained and shown in Fig. 13c and d. Compared with the results in Fig. 11a and d where constant turbine efficiencies are used, the net power output decreases slightly when the CNG engine works in the middle/high power regions. The energy efficiency can be improved by 8–11% under highway driving conditions.

The results showed that, the performance of the designed DORC system will drop when the operating point moving away from the optimal design point. The farther it is away from the design point, the lower the efficiency. Nevertheless, the engine will usually operate in a region relatively close to the optimal design point as

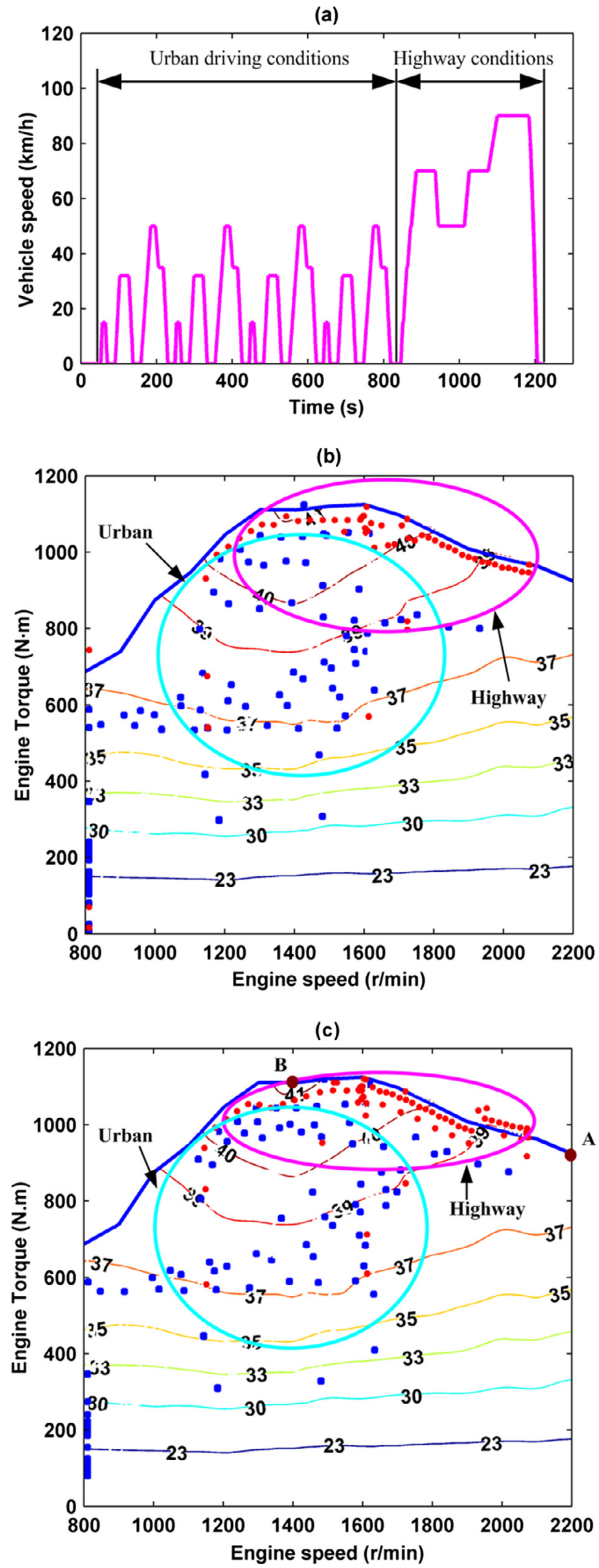

Fig. 12. Engine working points of a transit bus under different driving conditions: (a) the vehicle speed profile of ECE-EUDC-LOW driving cycle; (b) the engine working points with a 20% load weight; (c) the engine working points with a fully load weight.

highlighted in Fig. 12. The predicted efficiency improvement is still above 8% over this region.

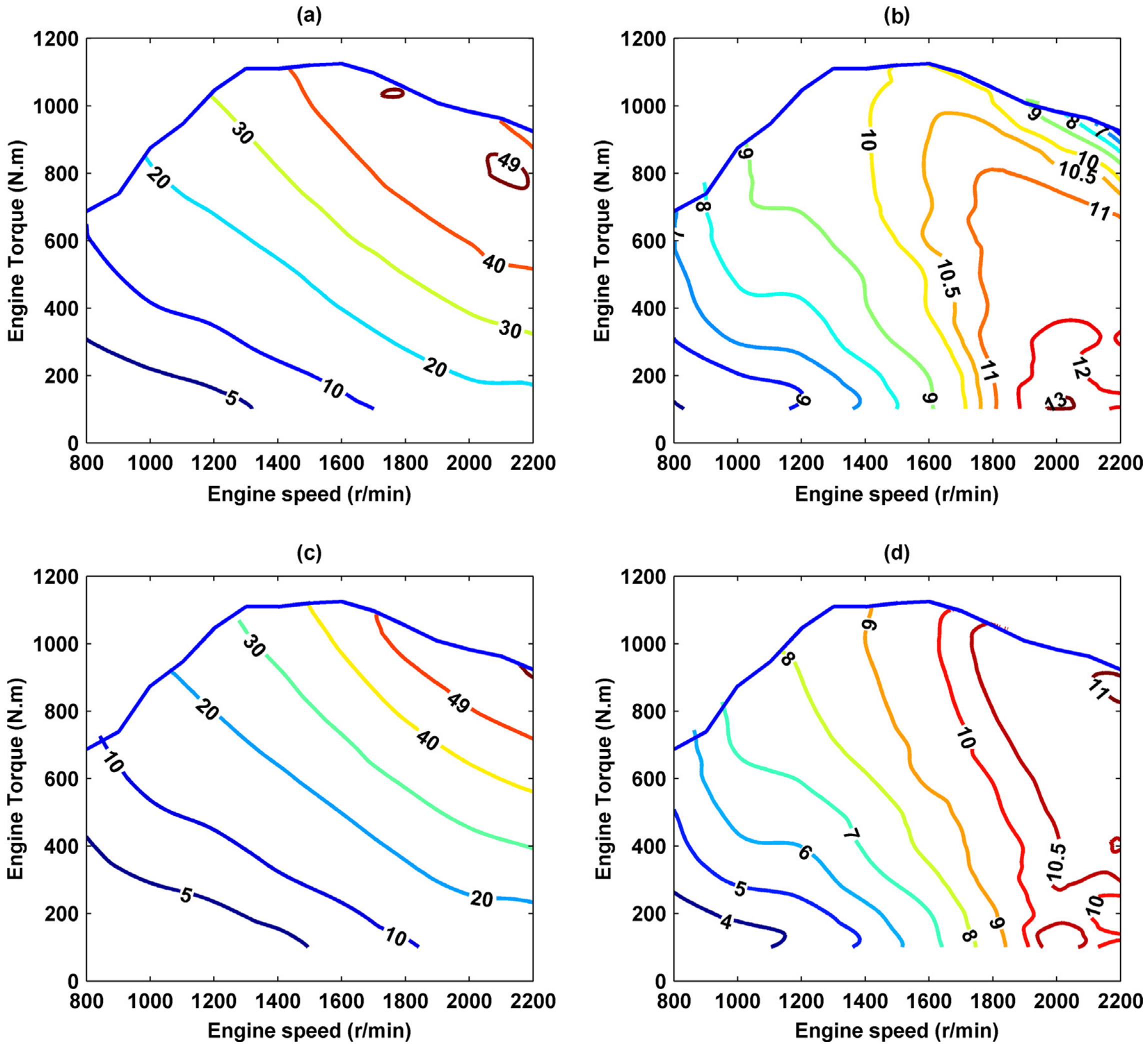

Fig. 13. Engine-DORC combined system performance with regard to off-design points: (a) the net power output of the DORC (kW) when Point B is the design point; (b) the absolute improvement of the effective thermal efficiency (%) when Point B is the design point; (c) the net power output of the DORC (kW) when Point A is the design point; (d) the absolute improvement of the effective thermal efficiency (%) when Point A is the design point.

However, like any other ORC systems energy recovery from engine's waste heat, the efficiency of the designed DORC system will be very low when the engine operates in a region that is too far from its normal operation point, such as start-up and idle. In practice, a bypass mechanism is needed to turn off the DORC system under these low-power operating conditions.

6.3. Effect of ambient temperature

A previous investigation indicated that the ambient temperature has a great impact on the performance of a DORC system [34]. For the proposed regenerative supercritical-subcritical DORC system, the condensation temperature of the LT loop can be changed with the ambient temperature. In this analysis, the engine speed is set as 1600 r/min and the engine torque is set as 600 N m. The net power output as a function of the ambient temperature is calculated and shown in Fig. 14a. The net power of the LT loop increases from 7 to 17 kW as the ambient temperature decreases from 35 °C to −5 °C while the net power output of the HT loop remains at 15.2 kW because the condensation temperature of the HT loop does not change when the ambient temperature varies. As a result, the net power output of the DORC increases from 22.2 kW to 32.2 kW. The power output of the combined engine-DORC system is increased from 123 kW to 133 kW as the ambient temperature decreases from 35 °C to −5 °C, as shown in Fig. 14b. The corresponding effective thermal efficiency of the combined system rises from 45.1% to 48.8%. In this study, the impact of the ambient temperature is obviously smaller than that of Ref. [34], because the heat transfer in the condenser of the LT loop of the proposed system has been significantly reduced due to the higher efficiency of the HT loop and the regenerator of the LT loop.

The SP of Turbine 2 as a function of the ambient temperature is shown in Fig. 14c. It increases from 1.26 to 1.47 as the ambient temperature decreases from 35 °C to −5 °C. However, the SP value of Turbine 1 keeps constant at 0.81. The required UA of the condenser versus the ambient temperature is given in Fig. 14d. It decreases from 10,284 to 9414 W/K as the ambient temperature drops. Therefore, the size of the turbine and condenser of the LT loop will be affected by the ambient temperature. In practice, the size of the turbine of the LT loop should be designed based on the minimum ambient temperature, while the heat transfer area of its condenser should be designed based on the maximum ambient temperature over a year.

In practice, the design point of the DORC system should be defined according to the driving conditions and the ambient temperature. The amount of waste heat from the CNG engine is used as an input parameter. The operating parameters of the DORC should be specified based on the results of Section 4. The sizes of

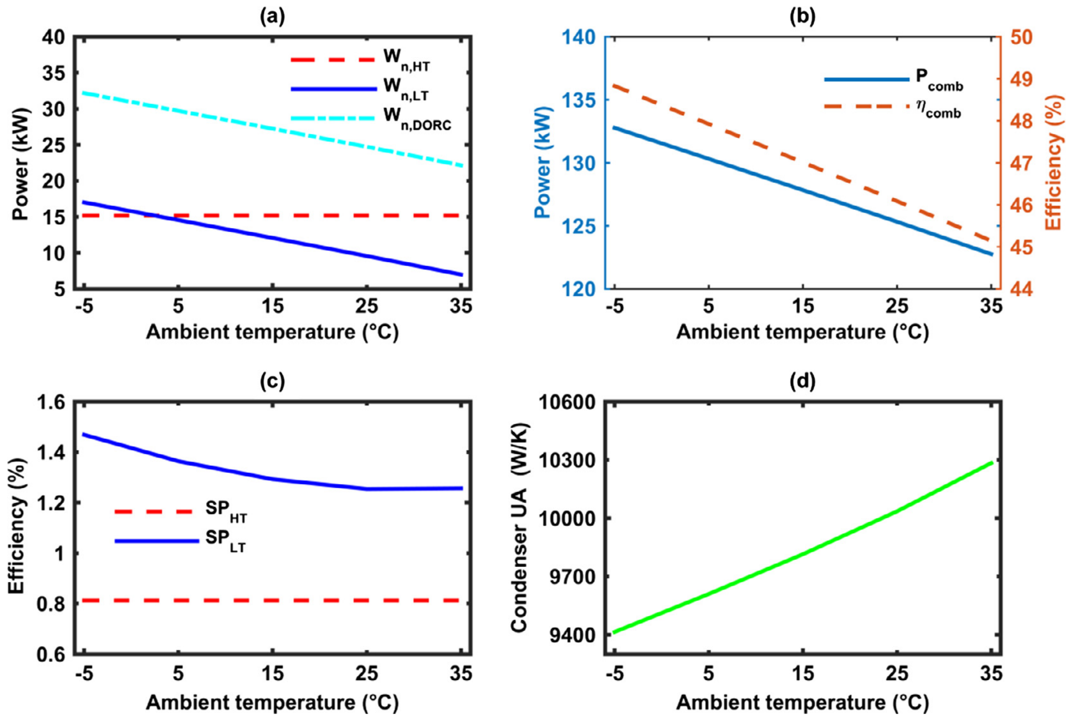

Fig. 14. Impact of the ambient temperature on the system performance when the engine operates at 1600 r/min and 600 N m: (a) the net power output of the HT and LT loops; (b) the net power and the effective thermal efficiency of the combined system; (c) the SP values of Turbines 1 and 2; (d) the UA of the condenser.

the turbines and heat exchangers can then be calculated. The designed DORC system can improve the energy efficiency when the engine operates around the design point.

7. Conclusion

In this paper, a regenerative supercritical-subcritical dual-loop ORC system is proposed to recover waste heat from both the exhaust gases and coolant of a CNG engine. The performance of the proposed cycle using four different pairs of working fluids has been analysed and compared in detail. The analysis has then been focused on the effect of regeneration and operational parameters such as turbine inlet pressure and temperature on the performance of the supercritical HT loop. Then, the performance of the engine-DORC combined system was evaluated.

Using a supercritical cycle can significantly improve the performance of the HT loop. For the supercritical HT loop using R1233zd or R245fa as working fluids, regeneration is beneficial only when the turbine inlet temperature is above a threshold value that strongly depends on the turbine inlet pressure. Increasing the turbine inlet temperature can improve the system's thermal efficiency noticeably, while increasing the turbine inlet pressure has little effect on the system's performance. For the HT loop using water, only a subcritical cycle is feasible but regeneration is not beneficial due to the relatively low temperature of the engine's waste heat.

Unlike other dual loop systems reported in literature [20], the net power output of the HT loop of the proposed system is higher than that of the LT loop, showing that a supercritical cycle is superior to a subcritical one for designing the HT loop. As such, the system becomes less sensitive to the fluctuation of ambient temperature.

When the proposed regenerative supercritical-subcritical DORC is coupled with a CNG engine, the design point should be selected based on the driving conditions. The simulations show that fuel efficiency can be improved by more than 8% for in most of the engine's operating regions. It is therefore inferred that the proposed regenerative supercritical-subcritical DORC system, together with other technologies such as combustion and gas flow optimisation, friction reduction, and electrically controlled pumps, could potentially improve the overall thermal efficiency of a CNG engine to around 55% as targeted by Department of Energy of the United States [33].

From the viewpoint of both the environmental friendliness and thermodynamic performance, among the four pairs of working fluids under consideration, R1233zd and R1234yf are believed to be the most suitable working fluids for the proposed regenerative supercritical-subcritical dual-loop ORC.

Acknowledgements

This research is funded by Royal Society (RG130051) and EPSRC (EP/N005228/1) in the United Kingdom, and a joint programme "Royal Society of the United Kingdom–National Natural Science Foundation of China (Ref: IE150866)".

Appendix A

In this section, the mathematical model for the regenerative supercritical-subcritical dual-loop ORC system is presented. For the regenerative supercritical HT loop, the power input of Pump 1 is expressed as

$$\dot{W}_{p1} = \dot{m}_{HT}(h_{HT2} - h_{HT1}) = \dot{m}_{HT}(h_{HT2s} - h_{HT1})/\eta_{p1}, \quad (A1)$$

The heat transfer within Regenerator 1 is represented by

$$Q_{r1} = m_{HT}(h_{HT3} - h_{HT2}) = m_{HT}(h_{HT5} - h_{HT4}). \quad (A2)$$

The evaporation process of the HT loop is

$$\dot{Q}_{e1} = \dot{m}_{exh}(h_{exh,in} - h_{exh,mid}) = \dot{m}_{HT}(h_{HT4} - h_{HT3}), \quad (A3)$$

In this study, various values for the temperature and pressure at state HT4 are specified. The enthalpy and other properties of state HT4 is computed by the state of equations using Refprop 9.1.

$$h_{HT4} = f(T_{HT4}, P_{HT4}) \tag{A4}$$

The power output of Turbine 1 is calculated as

$$\dot{W}_{t1} = \dot{m}_{HT}(h_{HT4} - h_{HT5}) = \dot{m}_{HT}\eta_{t1}(h_{HT4} - h_{HT5s}), \tag{A5}$$

The condensation process in the preheater is calculated by with

$$\dot{Q}_{pre} = \dot{m}_{HT}(h_{HT6} - h_{HT1}) = \dot{m}_{LT}(h_{LT5} - h_{LT4}), \tag{A6}$$

The net power output of the HT loop is calculated by

$$\dot{W}_{n,HT} = \dot{W}_{t1} - \dot{W}_{p1}. \tag{A7}$$

The thermal efficiency of the HT loop is determined by

$$\eta_{th,HT} = \frac{h_{HT4} - h_{HT5} + h_{HT1} - h_{HT2}}{h_{HT4} - h_{HT3}}. \tag{A8}$$

For a basic ORC without a regeneration, the thermal efficiency is then calculated as

$$\eta'_{th,HT} = \frac{h_{HT4} - h_{HT5} + h_{HT1} - h_{HT2}}{h_{HT4} - h_{HT2}}. \tag{A9}$$

For the LT loop, the power input of Pump 2 is calculated as

$$\dot{W}_{p2} = \dot{m}_{LT}(h_{LT2} - h_{LT1}) = \dot{m}_{LT}(h_{LT2s} - h_{LT1})/\eta_{p2}, \tag{A10}$$

The heat transfer in Regenerator 2 is expressed as

$$Q_{r2} = m_{LT}(h_{LT3} - h_{LT2}) = m_{LT}(h_{LT7} - h_{LT8}). \tag{A11}$$

The heat transfer in Evaporator 2 is calculated as

$$\dot{Q}_{e2} = \dot{m}_{LT}(h_{LT5} - h_{LT4}) = \dot{m}_{cool}(h_{cool,in} - h_{cool,out}), \tag{A12}$$

To ensure the temperature difference at the pinch point of Evaporator 2 is no less than 5 °C, the temperature at state LT5 must satisfy

$$T_{LT5} \leqslant T_{cool,in} - 5. \tag{A13}$$

The heat transfer in the superheater is expressed as

$$\dot{Q}_{s} = \dot{m}_{exh}(h_{exh,mid} - h_{exh,out}) = \dot{m}_{LT}(h_{LT6} - h_{LT5}). \tag{A14}$$

The power output of Turbine 2 is

$$\dot{W}_{t2} = \dot{m}_{LT}(h_{LT6} - h_{LT7}) = \dot{m}_{LT}\eta_{t2}(h_{LT6} - h_{LT7s}), \tag{A15}$$

The heat transfer in the condenser is computed as

$$\dot{Q}_{c} = \dot{m}_{LT}(h_{LT8} - h_{LT1}). \tag{A16}$$

The net power output of the LT loop is

$$\dot{W}_{n,LT} = \dot{W}_{t2} - \dot{W}_{p2}. \tag{A17}$$

The thermal efficiency of the LT loop is defined as

$$\eta_{th,LT} = \frac{h_{LT6} - h_{LT7} + h_{LT1} - h_{LT2}}{h_{LT6} - h_{LT3}}. \tag{A18}$$

If a basic ORC is used for the LT loop, the thermal efficiency is

$$\eta'_{th,LT} = \frac{h_{LT6} - h_{LT7} + h_{LT1} - h_{LT2}}{h_{LT6} - h_{LT2}}. \tag{A19}$$

The total net power output of the regenerative supercritical-subcritical DORC system is

$$\dot{W}_{n,DORC} = \dot{W}_{n,HT} + \dot{W}_{n,LT}. \tag{A20}$$

The effective thermal efficiency of the engine can be defined as

$$\eta_{th,eng} = \frac{\dot{W}_{n,eng}}{\dot{m}_f H_f}, \tag{A21}$$

The thermal efficiency of the engine-ORC combined system is determined by

$$\eta_{th,comb} = \frac{\dot{W}_{n,eng} + \dot{W}_{n,HT} + \dot{W}_{n,LT}}{\dot{m}_f H_f}. \tag{A22}$$

References

[1] Saidur R, Rezaei M, Muzammil WK, Hassan MH, Paria S, Hasanuzzaman M. Technologies to recover exhaust heat from internal combustion engines. Renew Sustain Energy Rev 2012;16:5649–59.
[2] Temizer I, İlkılıç C. The performance and analysis of the thermoelectric generator system used in diesel engines. Renew Sustain Energy Rev 2016;63:141–51.
[3] Zhang J, Cho H, Knizley A. Evaluation of financial incentives for combined heat and power (CHP) systems in U.S. regions. Renew Sustain Energy Rev 2016;59:738–62.
[4] Karvonen M, Kapoor R, Uusitalo A, Ojanen V. Technology competition in the internal combustion engine waste heat recovery: a patent landscape analysis. J Clean Prod 2016;112:3735–43.
[5] Agudelo AF, García-Contreras R, Agudelo JR, Armas O. Potential for exhaust gas energy recovery in a diesel passenger car under European driving cycle. Appl Energy 2016;174:201–12.
[6] Mondejar ME, Ahlgren F, Thern M, Genrup M. Quasi-steady state simulation of an organic Rankine cycle for waste heat recovery in a passenger vessel. Appl Energy 2016. http://dx.doi.org/10.1016/j.apenergy.2016.03.024.
[7] Wang EH, Zhang HG, Fan BY, Ouyang MG, Zhao Y, Mu QH. Study of working fluid selection of organic Rankine cycle (ORC) for engine waste heat recovery. Energy 2011;36:3406–18.
[8] Li J, Li P, Pei G, Alvi JZ, Ji J. Analysis of a novel solar electricity generation system using cascade Rankine cycle and steam screw expander. Appl Energy 2016;165:627–38.
[9] Braimakis K, Preißinger M, Brüggemann D, Karellas S, Panopoulos K. Low grade waste heat recovery with subcritical and supercritical organic Rankine cycle based on natural refrigerants and their binary mixtures. Energy 2015;88:80–92.
[10] Larsen U, Pierobon L, Haglind F, Gabrielii C. Design and optimisation of organic Rankine cycles for waste heat recovery in marine applications using the principles of natural selection. Energy 2013;55:803–12.
[11] Le VL, Feidt M, Kheiri A, Pelloux-Prayer S. Performance optimization of low-temperature power generation by supercritical ORCs (organic Rankine cycles) using low GWP (global warming potential) working fluids. Energy 2014;67:513–26.
[12] Freeman J, Hellgardt K, Markides CN. Working fluid selection and electrical performance optimisation of a domestic solar-ORC combined heat and power system for year-round operation in the UK. Appl Energy 2016. http://dx.doi.org/10.1016/j.apenergy.2016.04.04.
[13] Toffolo A, Lazzaretto A, Manente G, Paci M. A multi-criteria approach for the optimal selection of working fluid and design parameters in organic Rankine cycle systems. Appl Energy 2014;121:219–32.
[14] Yang MH, Yeh RH. Thermodynamic and economic performances optimization of an organic Rankine cycle system utilizing exhaust gas of a large marine diesel engine. Appl Energy 2015;149:1–12.
[15] Shu G, Li X, Tian H, Liang X, Wei H, Wang X. Alkanes as working fluids for high-temperature exhaust heat recovery of diesel engine using organic Rankine cycle. Appl Energy 2014;119:204–17.
[16] Di Battista D, Mauriello M, Cipollone R. Waste heat recovery of an ORC-based power unit in a turbocharged diesel engine propelling a light duty vehicle. Appl Energy 2015;152:109–20.
[17] Song J, Song Y, Gu C. Thermodynamic analysis and performance optimization of an organic Rankine cycle (ORC) waste heat recovery system for marine diesel engines. Energy 2015;82:976–85.
[18] Kim YM, Shin DG, Kim CG, Cho GB. Single-loop organic Rankine cycles for engine waste heat recovery using both low- and high-temperature heat sources. Energy 2016;96:482–94.
[19] Freymann R, Strobl W, Obieglo A. The turbosteamer: a system introducing the principle of cogeneration in automotive applications. MTZ 2008;69:404–12.
[20] Wang EH, Zhang HG, Zhao Y, Fan BY, Wu YT, Mu QH. Performance analysis of a novel system combining a dual loop organic Rankine cycle (ORC) with a gasoline engine. Energy 2012;43:385–95.
[21] Zhang HG, Wang EH, Fan BY. A performance analysis of a novel system of a dual loop bottoming organic Rankine cycle (ORC) with a light-duty diesel engine. Appl Energy 2013;102:1504–13.
[22] Yang K, Zhang H, Wang Z, Zhang J, Yang F, Wang E, et al. Study of zeotropic mixtures of ORC (organic Rankine cycle) under engine various operating conditions. Energy 2013;58:494–510.
[23] Shu G, Liu L, Tian H, Wei H, Liang Y. Analysis of regenerative dual-loop organic Rankine cycles (DORCs) used in engine waste heat recovery. Energy Convers Manage 2013;76:234–43.
[24] Shu G, Liu L, Tian H, Wei H, Xu X. Performance comparison and working fluid analysis of subcritical and transcritical dual-loop organic Rankine cycle (DORC) used in engine waste heat recovery. Energy Convers Manage 2013;74:35–43.
[25] Maraver D, Royo J, Lemort V, Quoilin S. Systematic optimization of subcritical and transcritical organic Rankine cycles (ORCs) constrained by technical parameters in multiple applications. Appl Energy 2014;117:11–29.

[26] Glover S, Douglas R, De Rosa M, Zhang X, Glover L. Simulation of a multiple heat source supercritical ORC (organic Rankine cycle) for vehicle waste heat recovery. Energy 2015;93:1568–80.
[27] Tian H, Liu L, Shu G, Wei H, Liang X. Theoretical research on working fluid selection for a high-temperature regenerative transcritical dual-loop engine organic Rankine cycle. Energy Convers Manage 2014;86: 764–73.
[28] Ouyang M, Zhang W, Wang E, Yang F, Li J, Li Z, et al. Performance analysis of a novel coaxial power-split hybrid powertrain using a CNG engine and supercapacitors. Appl Energy 2015;157:595–606.
[29] Yao B, Yang F, Zhang H, Wang E, Yang K. Analyzing the performance of a dual loop organic Rankine cycle system for waste heat recovery of a heavy-duty compressed natural gas engine. Energies 2014;7:7794–815.
[30] Angelino G, Invernizzi C, Macchi E. Organic working fluid optimization for space power cycles. In: Angelino G, De Luca L, Sirignano WA, editors. Modern research topics in aerospace propulsion. Springer-Verlag; 1991. p. 297–324.
[31] Macchi E, Perdichizzi A. Efficiency prediction for axial-flow turbines operating with nonconventional fluids. J Eng Power Trans ASME 1981;103:718–24.
[32] Manente G, Toffolo A, Lazzaretto A, Paci M. An organic Rankine cycle off-design model for the search of the optimal control strategy. Energy 2013;58:97–106.
[33] Salemme G. Emerging engine technologies for heavy duty vehicle fuel efficiency. In: ACEEE-ICCT workshop. July 22 http://aceee.org/conferences/2014/workshop.
[34] Wang EH, Zhang HG, Fan BY, Ouyang MG, Yang FY, Yang K, et al. Parametric analysis of a dual-loop ORC system for waste heat recovery of a diesel engine. Appl Therm Eng 2014;67:168–78.